Proceedings of the Federated Conference on
Computer Science and Information Systems pp. 693–700

DOI: 10.15439/2015F208
ACSIS, Vol. 5

Trigger Based on the Artificial Neural Network implemented in the Cyclone V FPGA for a Detection of Neutrino-Origin Showers in the Pierre Auger surface detector

Zbigniew Szadkowski
Dariusz Głas
University of Łódź
Department of Physics and Applied Informatics
Faculty of High-Energy Astrophysics
E-mail : zszadkow@kfd2.phys.uni.lodz.pl
E-mail : dglas@uni.lodz.pl

Krzysztof Pytel
University of Łódź
Department of Physics and Applied Informatics
90-236 Łódź, Pomorska 149
Faculty of Informatics
Email : kpytel@uni.lodz.pl

***Abstract*—Observations of ultra-high energy neutrinos became a priority in experimental astroparticle physics. Up to now, the Pierre Auger Observatory did not find any candidate on a neutrino event. This imposes competitive limits to the diffuse flux of ultra-high energy neutrinos in the EeV range and above.**

The prototype Front-End boards for Auger-Beyond-2015 with Cyclone® V E can test the neural network algorithm in real pampas conditions in 2015. Showers for muon and tau neutrino initiating particles on various altitudes, angles and energies were simulated in CORSIKA and OffLine platforms giving pattern of ADC traces in Auger water Cherenkov detectors. The 3-layer 12-10-1 neural network was taught in MATLAB by simulated ADC traces according the Levenberg - Marquardt algorithm. New sophisticated trigger implemented in Cyclone® V E FPGAs with large amount of DSP blocks, embedded memory running with 120 - 160 MHz sampling may support to discover neutrino events in the Pierre Auger Observatory.

I. Introduction

OBSERVATION of ultrahigh energy cosmic rays (UHECR) of energy $1-100$ EeV ($10^{18} - 10^{20}$ eV) has stimulated much experimental as well as theoretical activity in the field of astro-particle Physics [1]. Although many mysteries remain to be solved, such as the origin of the UHECRs, their production mechanism and composition, we know that it is very difficult to produce these energetic particles without associated fluxes of ultrahigh energy neutrinos (UHEνs) [2]. In the "bottom-up" scenarios, protons and nuclei are accelerated in astrophysical shocks, while pions are produced by cosmic ray interactions with matter or radiation at the source [3]. In the "top-down" models, protons and neutrons are produced from quark and gluon fragmentation with a production of much more pions than nucleons [4]. Furthermore, protons and nuclei also produce pions due to the Greisen-Zatsepin-Kuzmin (GZK) cutoff [5]. The ultrahigh energy cosmic rays (UHECR) flux above $\sim 5\times10^{19}$ eV is significantly suppressed according to expectations based on the UHECRs interaction of with the cosmic microwave background (CMB) radiation [6]. For primary protons, the photo-pion production is responsible for the GZK effect, thus UHEνs are produced from decayed charged pions. However, their fluxes are doubtful [4] and if the primaries are heavy nuclei, the UHEνs should be strongly suppressed [7].

Neutrinos can show directly sources of their production due to no deflection by magnetic fields. Unlike photons they travel inviolate from the sources carrying an impression of the production model. UHEνs can be detected with arrays of detectors at ground level that are currently being used to measure extensive showers produced by cosmic rays [8]. The main challenge is an extraction from the background, induced by regular cosmic rays, showers initiated by neutrinos. Due to a very small neutrino cross-section for interactions, higher probability of a detection is at high zenith angles [9] due to a bigger atmosphere slant depth provides thicker target for neutrino interactions. Inclined showers starting a development deeply in the atmosphere can be a signature of neutrino events.

II. Triggers

Each water Cherenkov detector of the surface array has a 10 m^2 water surface area and 1.2 m water depth, with three 9-inch photomultiplier tubes (PMTs) looking through optical coupling material into the water volume, which is contained in a Tyvek reflective liner. Each PMT provides signals, which are digitized by 40 MHz 10-bit Analog to Digital Converters (ADCs).

Triggers are generated for signals above amplitude thresholds. The trigger for the surface detector array is hierarchical. Two levels of trigger (called T1 and T2) are formed at each detector. T2 triggers are combined with those from other detectors and examined for spatial and temporal correlations, leading to an array trigger (T3). The T3 trigger initiates data acquisition and storage. Two independent trigger modes are

978-83-60810-66-8/$25.00

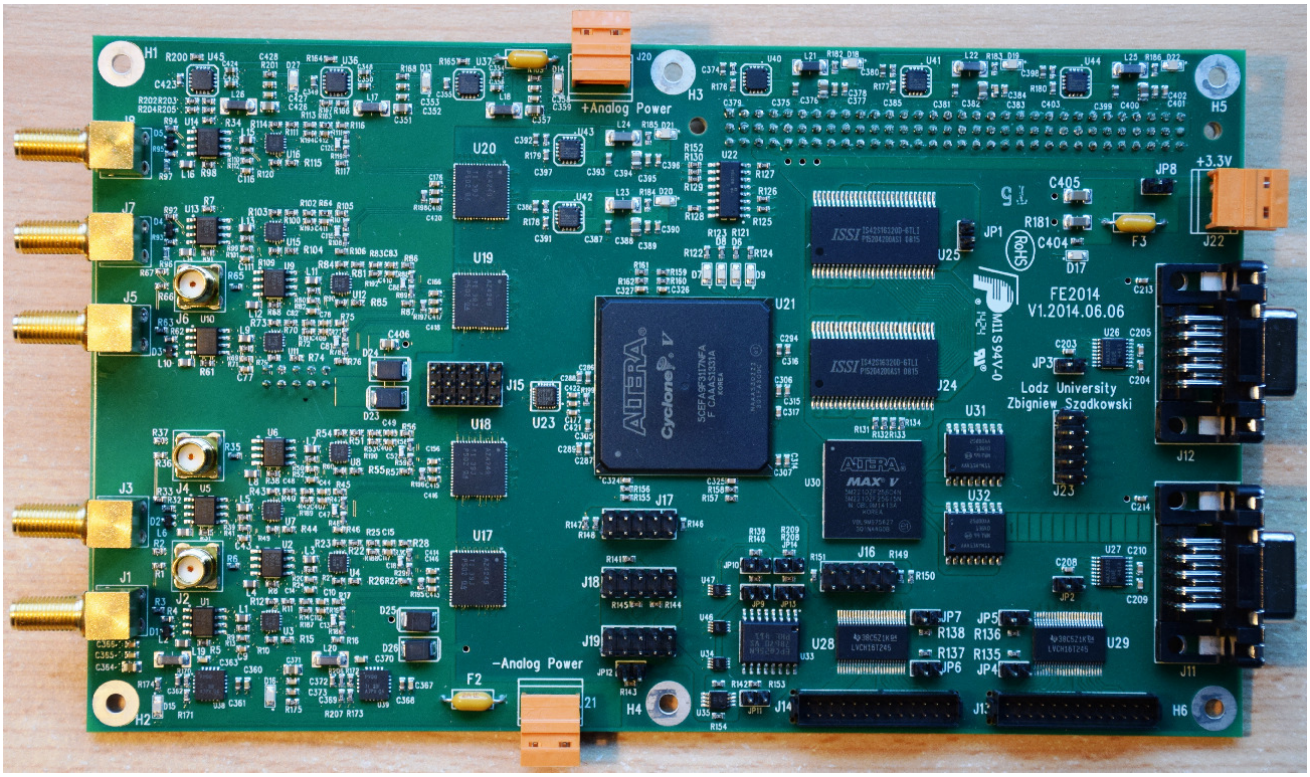

Fig. 1. The Front-End Board developed for the Auger-Beyond-2015 upgrade design used also for the ANN algorithm tests.

implemented as T1. The 1st T1 mode is a simple threshold trigger (TH) which requires the coincidence of the three PMTs each above 1.75 I_{VEM}^{peak}. The Vertical Equivalent Muon (VEM) is a unit used for a calibration corresponding to ∼50 ADC-units for 40 MHz sampling frequency. This trigger is used to select large signals that are rather concentrated in time. The 2nd mode is designated the "Time-over-Threshold" trigger (ToT) and at least 13 time-bins in 120 ADC bins of a sliding window of 3 μs are required to be above a threshold of 0.2 I_{VEM}^{peak} in coincidence in 2 out of 3 PMTs. This trigger is intended to select sequences of small signals spread in time. From the point of view of short pulses characteristic for very inclined "old" showers as well as for relatively short signals for inclined "young showers the ToT trigger is useless.

FPGAs currently used in the Pierre Auger surface detectors analyze signal amplitudes in a time domain. Much higher efficiency can provide spectral triggers based i.e. on Discrete Cosine Transform [10] [11] [12]. Triggers based on an artificial neuron networks is an alternative approach focusing on specific patterns of ADC traces registered in Pierre Auger water Cherenkov detectors [13].

III. ADC TRACES ANALYSIS

With the SD of the Pierre Auger Observatory we can detect and identify UHE neutrinos in the EeV range and above [14]. Due to much larger cross-section than neutrinos, the 1st interaction for protons, heavier nuclei and even photons usually appears shortly after entering the atmosphere. However, neutrinos can generate showers initiated deeply into the atmosphere. Vertical showers initiated by protons or heavy nuclei have a considerable amount of electromagnetic component at the ground ("young" shower front). However, at high zenith angles ($\theta \geq 75$) (thicker than about three vertical atmospheres), UHECRs interacting high in the atmosphere generate shower fronts dominated by muons at ground ("old" shower front), which generate narrow signals (short ADC traces) spreading over typically tens of nano-seconds in practically all the stations of the event. These traces can be recognized with 16-point DCT algorithm as well as with 16-point input AAN.

Calculations show [15] that "young" showers are spread in time over hundreds of nano-seconds. For the "old" showers practically only the muonic components survives. It gives a short bump in the SD. The "young" showers contains also some electromagnetic component, which enlarge in time an ADC traces. However, muonic components of "young" showers is ahead of the electromagnetic one and gives an early bump. The rising edge of the bump is not so sharp as for the "old" ones, but the signal next is also relatively fast attenuated, till the electromagnetic component starts to give its own contribution. The ANN approach can focus on the early bump, to select traces potentially generated by neutrinos.

On the other hand, independent simulations of showers in CORSIKA [16] an next calculation of water Cherenkov detectors (WCDs) response in OffLine package [17] showed

TABLE I
DISTANCES FROM THE PLACE OF THE FIRST INTERACTION TO DETECTOR FOR PROTONS AND MUON NEUTRINOS IN DEPENDENCE OF ZENITH ANGLE. ALL THE DISTANCES ARE IN g/cm^2. BECAUSE OF THE GEOMETRY NOT ALL THE DISTANCES ARE AVAILABLE FROM EVERY ANGLE.

		500	1000	2000	3000	4000	5000	10000
80°	p			+	+	+		
80°	ν	+	+	+	+	+		
85°	p			+	+	+	+	
85°	ν	+	+	+	+	+	+	
89°	p			+	+	+	+	+
89°	ν	+	+	+	+	+	+	+

that for neutrino showers (initiated either by ν_μ or ν_τ) for relatively big zenith angle (i.e. 70°) and low altitude (9 km) (to be treated as "young" showers before a maximum of development) give relatively short ADC traces and they can be analyzed also by 16-point pattern engines [13].

IV. CORSIKA AND OFFLINE CALCULATIONS

The main motivation of an ANN implementation as a shower trigger is a fact that up to now the entire array did not registered any neutrino-induced event. The probably reasons are: a) a very low stream of neutrinos and b) amplitudes of ADC-traces are small and probably are below of threshold of standard 3-fold coincidence trigger. The main idea was to use ANN approach as a pattern recognition technique.

The input data for the ANN are simulated traces of protons and muon neutrinos, which hit the atmosphere in high zenith angles - 80°, 85° and 89°, respectively. The chosen energies of primary particles are 3×10^8, 10^9, 3×10^9 and 10^{10} GeV, respectively. The distances from the place of the first interaction to the detector used for simulations are dependent of the angle and the type of particle (Table I). We decided not to simulate protons which are very close to detector, because the probability that proton will not interact on long way to detector is very low. Additionally, traces produced by this kind of interactions may include also electromagnetic part of the shower. These traces would look completely different than the rest and may significantly decrease the efficiency of the ANN.

There are 120 different categories. These categories are used as input by the CORSIKA simulation platform. The CORSIKA program simulates the cosmic ray shower initiated by the specific particle. The result of this simulation is distribution of the position and energies of the particles on the level of the detector. Simulations are relatively fast. All of the 120 categories had been simulated in a week. The simulated cosmic ray showers are the input for the OffLine package, which provides a response of the water Cherenkov detector and generates the ADC traces (signal waveforms). These simulations are very time consuming. As a result we got simulated traces from the photo-multipliers, as if they were triggered by standard T1 trigger. We have proven that 16-point input is sufficient for the ANN pattern recognition [13]. The next step was to find in the 16-point trace, which corresponds to triggered events. To clearly see the beginning of the event we decided that two first points should be on the pedestal level. Afterwards we subtracted the pedestal level from all used data. These extracted points we could finally use for training and testing our neural network.

For a training procedure, we decided to use half of the data available for the testing procedure. We arrange data, to have proton and neutrino traces alternately. The proton traces were treated as negative signals ("0" for the ANN) and the neutrino traces were treated as positive ones ("1" for the ANN). This step allowed the ANN to teach faster and get less errors while training. The testing procedure consists on assigning specific value to the trace. This value depends on the coefficients of the trained ANN. If the value is greater than the threshold, the trace is treated as a neutrino trace, otherwise it is treated as a proton trace. The efficiency of the neutrino recognition with specific threshold level can be defined as number of neutrino traces recognized correctly divided by the number of all neutrino traces. The proton mistakes level is defined as number of proton traces treated as neutrino traces divided by the number of all proton traces.

The testing procedure was divided into two stages. First, we wanted to find out if we could use the data from the specific category to distinguish muon neutrinos and protons for all the angles or all the energies. Simulated data contains only three different angles: 80°, 85° and 89°, respectively, but we do not expect the zenith angle of the particle would be exactly like them. If the ANN trained on the specific category with angle 85° can distinguish neutrinos and protons also for 89° and 80° with acceptable efficiency, we assumed it could distinguish protons and neutrinos also for full angle range: 80° - 89°. The same is for energies. The ANN had been also trained by the data of the specific energy and then it was tested on the other values of the chosen parameter. The second step of the testing procedure consisted on training the ANN by the randomly taken data from all categories. In this case we used 30% of the whole data for training the ANN. The result from this step should be better than in previous one, because the data used for teaching was taken from the wider set of data.

The efficiency of the ANN strongly depends on the data used for training. The positive and negative signals should be as different as possible, to increase the distinction of proton and neutrino traces. Our first results (Fig. 9 continuous line) shows, that ANN does not work properly. There was no separation between protons and neutrinos. When we looked at the data we used for teaching the ANN, we found that some of the neutrino and proton traces looked very similar to each other. Moreover the simulated traces produced by neutrino shower with various distances to the detector, but with the same energy and angle was diametrically different. The same effect we observed in the other angles and energies (Fig. 2) and in the traces produced by protons (Fig. 7). This effect is directly connected with the electromagnetic (EM) part of the shower. If the distance to the detector is short, the EM part of the shower gives second component in the traces, additional to standard muonic one. At high zenith angles the proton showers should not have the EM component, because it should disappear after 2000 - 3000 g/cm^2. Old

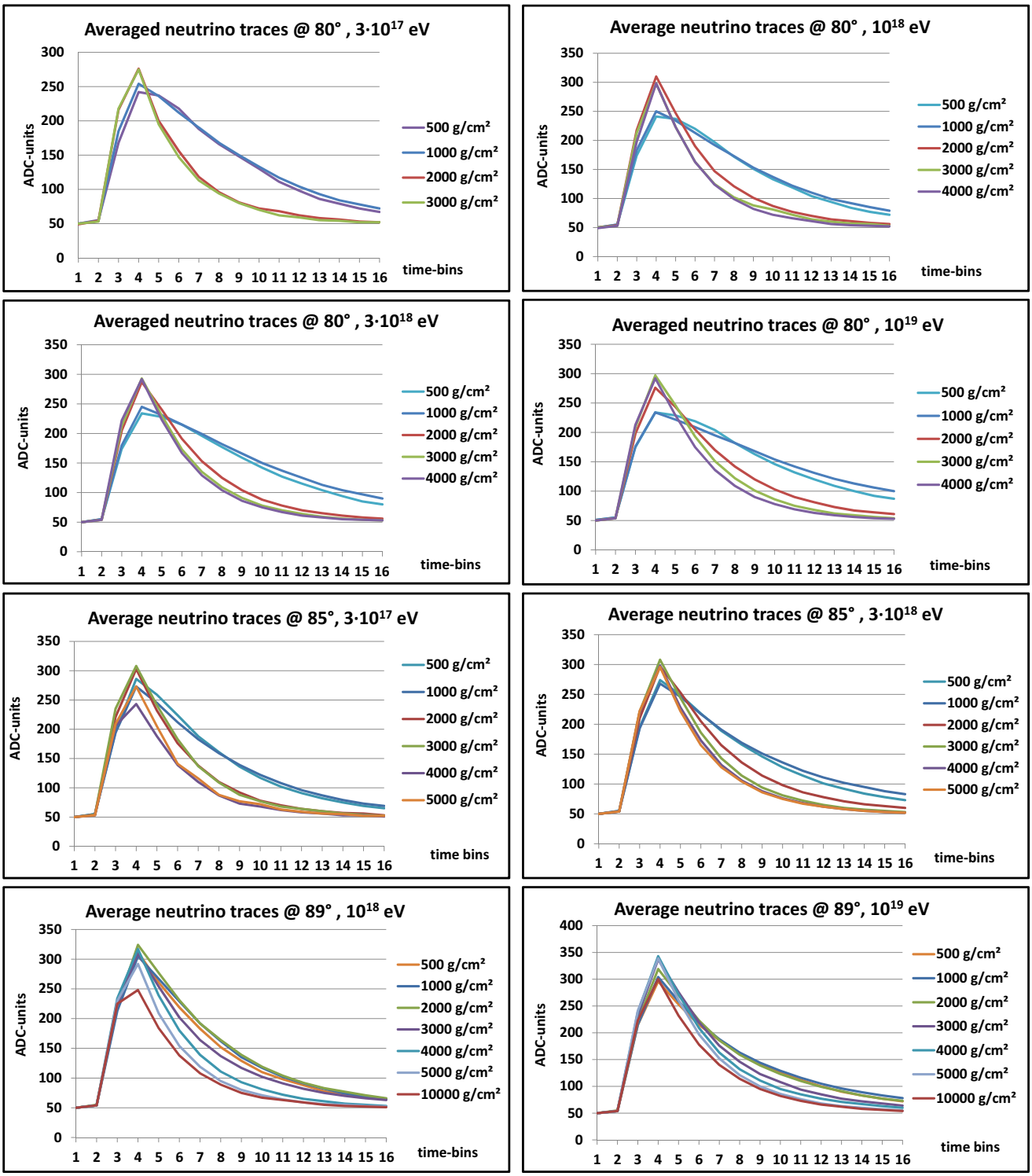

Fig. 2. Plots contain averaged neutrino signal waveforms (ADC traces) for various angles, energies and initialization points. The exponents of the traces at distances 500 and 1000 g/cm^2 are different than on the rest of distances. This effect does not depends on the energy and slightly depends on the angle.

neutrino showers looked like old proton neutrino showers, so we decided to separate the data and focus on recognizing only the young neutrino showers, where the EM component was still visible. We also decided to remove proton showers with visible EM component, because traces they generated looked similar to traces generated by young neutrino showers.

Moreover, for this showers the probability to occur on this angles was low. The data we decided to keep were all neutrino traces with distances 500 and 1000 g/cm^2 and all proton traces with two maximal distances for each angle. Fig. 5 shows the average traces for data at 80° after the separation. Neutrino and proton traces have completely different shapes and it would be easier to recognize the neutrino traces when ANN is learned and tested on this data. Fig. 6 shows the histogram of the average exponents of rejected and accepted proton and neutrino categories. We can observe that the exponents of the rejected neutrino categories corresponds with exponents of the accepted proton categories. This was probably the main reason of low distinction of protons and neutrinos by ANN. Additionally, average exponents of the accepted proton and neutrino categories are separated.

V. MATLAB ANALYSIS

On Fig. 8a we can see how the angular efficiency behaves. In the case, when the ANN was tested on all categories, the ANN was learned using the specific category with parameters: angle 85°, energy 3×10^{18} eV, distance to detector 2000 g/cm^2

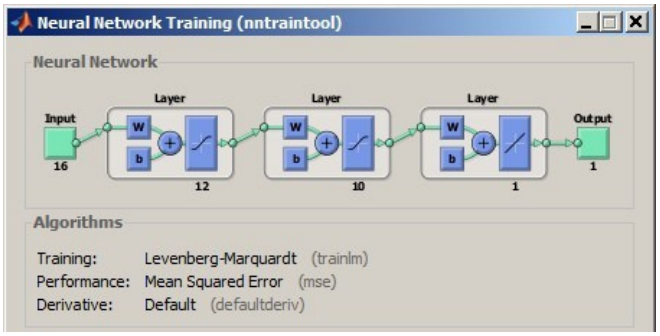

Fig. 3. An example of the ANN structure used for an optimization in Neutral Network Training of the MATLAB toolbox.

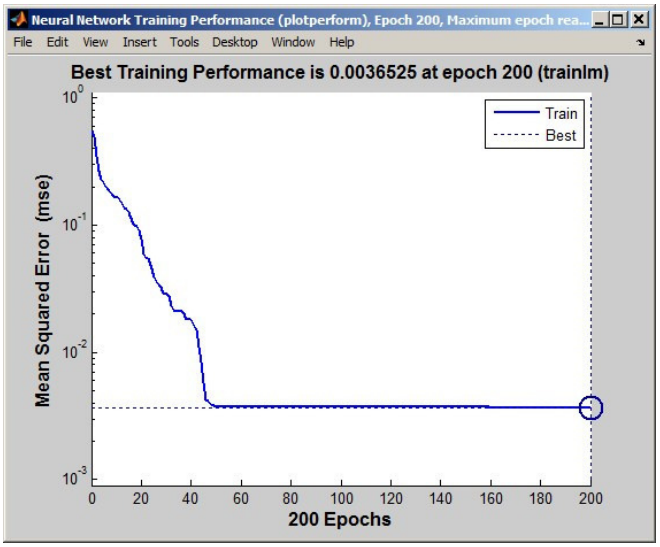

Fig. 4. Training performance for the 3-layer network 12-10-1

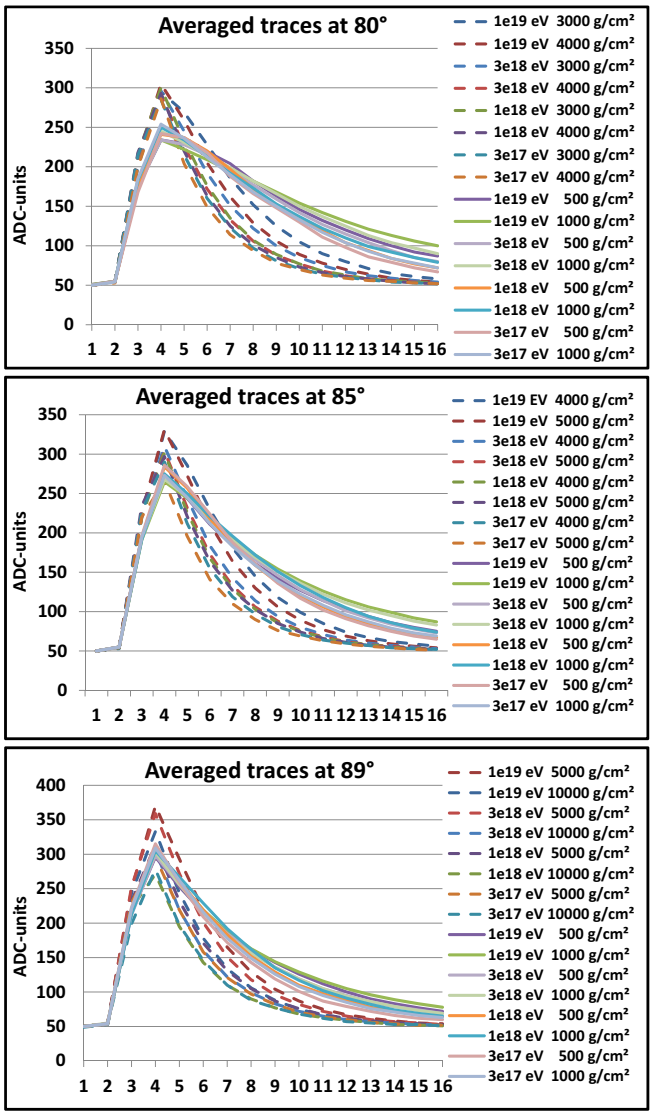

Fig. 5. The plot showing the differences between the traces produced by old proton showers (dashed line) and young neutrino showers (continuous line).

both for protons and neutrinos. The separated case used 80°, 3×10^{18} eV and 500 g/cm^2 as positive signals (neutrinos) and 80°, 3×10^{18} eV and 4000 g/cm^2 as negative signals (protons). For the case, which use all categories for tests, the efficiency seems to be independent of the angle. The case, which use only traces produced by young neutrino and old proton showers ("separated" case) shows the efficiency changes slightly, when we change the angle. On Fig. 8b we can see that in both cases the efficiency of the ANN is independent of the energy (in the used energy range). Fig. 9 shows the comparison between both cases. The ANN tested on non-separated traces has problems with distinguishing the proton and neutrinos on every level of the threshold. The effectiveness of finding neutrino traces and the level of proton mistakes differs only slightly. The second ANN, tested on the separated traces, can recognize protons

and neutrinos with acceptable efficiency. The proton mistakes level is much lower than efficiency of finding the neutrino traces, moreover the efficiency of finding neutrino traces is higher than in the previous case. Finally, Fig. 10 shows the difference of the non-separated and separated cases, when the data taken for training the ANN was taken randomly from all traces, appropriate for specific case. We can see that, the distinguishing the proton and neutrino traces increased in both cases, but the recognition of the neutrinos and protons is much better when we teach the ANN with the data from separated traces. In this case the neutrino efficiency to proton mistakes level ratio is greater than two, when in the other case this ratio is on the level of 1.3. This ratio is very important, because it shows if the ANN works or not. The ratio on the level of one means the ANN does not work, because the neutrino to proton traces quotient is the same as in the whole data. The data triggered as neutrino would be processed off-line in next steps. Lower level of proton mistakes and greater efficiency of recognizing neutrino traces means that amount of data to process off-line would be smaller, but neutrino traces would appear more frequently in it.

VI. FPGA Implementation

A 16-input neuron for 14-bit data and 14-bit coefficients is shown on Fig. 11. An neuron output drives a neural transfer function - a tansig, which calculates a layer output from its net input. It can be implemented as ROM in embedded FPGA memory. We selected 14-bit input, 14-bit-output tansig implementation in RAM: a 2-port function with blocked writing left port to keep a reasonable compromise between a calculation accuracy and a memory size. The same array of coefficients is used for two independent neuron transfer functions.

The 12-10-1 network (Fig. 3) offers the best performance (Fig. 4) with a minimal resource occupancy, however, it requires 23 neurons. Due to the limited amount of DSP blocks, we could use this network for a single PMT only. The Quartus compiler allows a compilation with arbitrarily selected implementations of the multipliers: either in the DSP blocks or in logic elements only. An implementation of the multipliers in the Adaptive Logic Modules (ALMs) is much more resource-consuming (1247 ALMs instead of 107 ALMs + 8 DSP blocks). However, such a selection allows the implementation of a more complicated network, which provides a similar registered performance (keeps approximately the same speed). The 3-channel 12-10-1 network needs 36 neurons (1st layer implemented in the DSP blocks) + 33 neurons implemented in 41151 ALMs (36.5% of 5CEFA9F31I7).

VII. Conclusion

We run CORSIKA simulation for proton, iron, ν_μ and ν_τ primaries. Output data collected on 1450 m (the level of the Pierre Auger Observatory) was an input for OffLine providing the ADCs response in the WCDs. Obtained ADC traces were thus used to teach the 12-10-1 neural network implemented already in the 5CEFA7F31I7 FPGA on the Cyclone® V development kit. This FPGA is smaller version of the chip

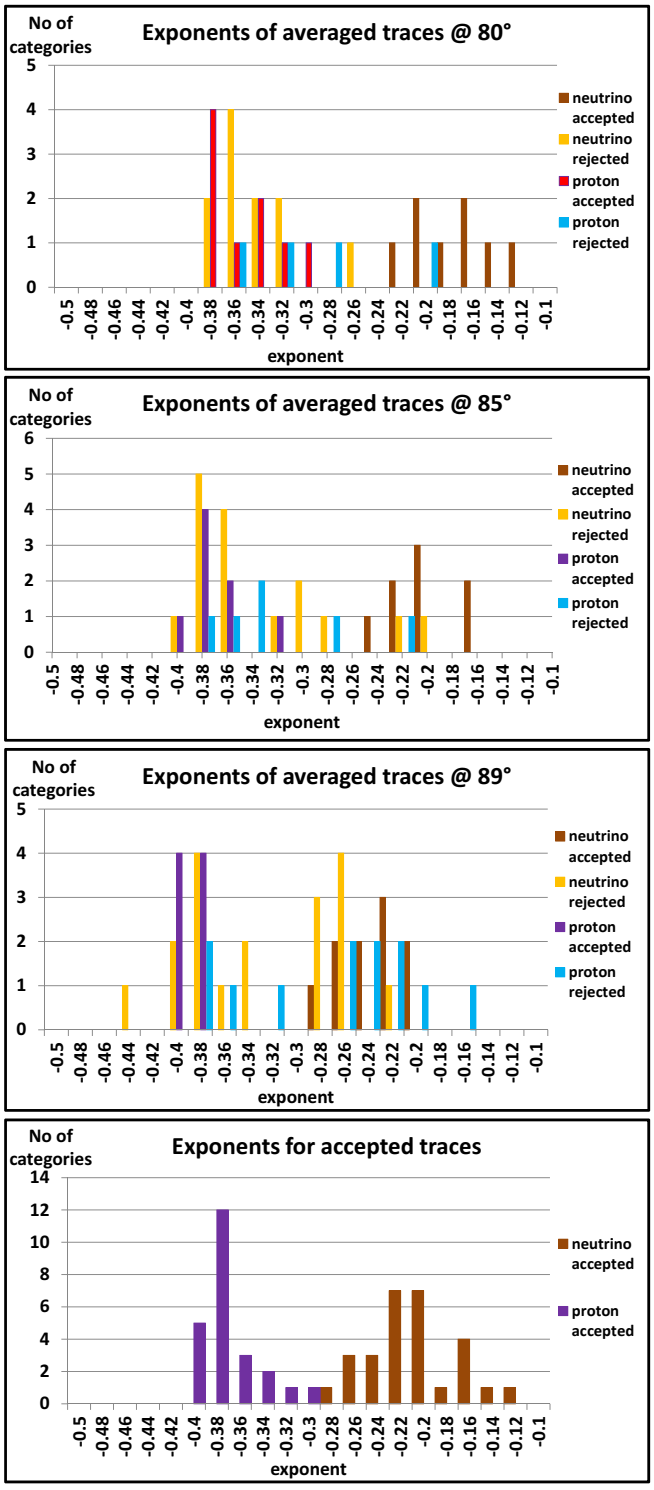

Fig. 6. A histogram of exponents of rejected and accepted traces for protons and neutrinos. The accepted neutrino traces exponents are separated from the accepted proton traces exponents. The rejected neutrino traces looks very similar like traces made by old proton showers. This may cause problems with ANN training and may increase the level of the proton traces recognized as neutrino traces by ANN.

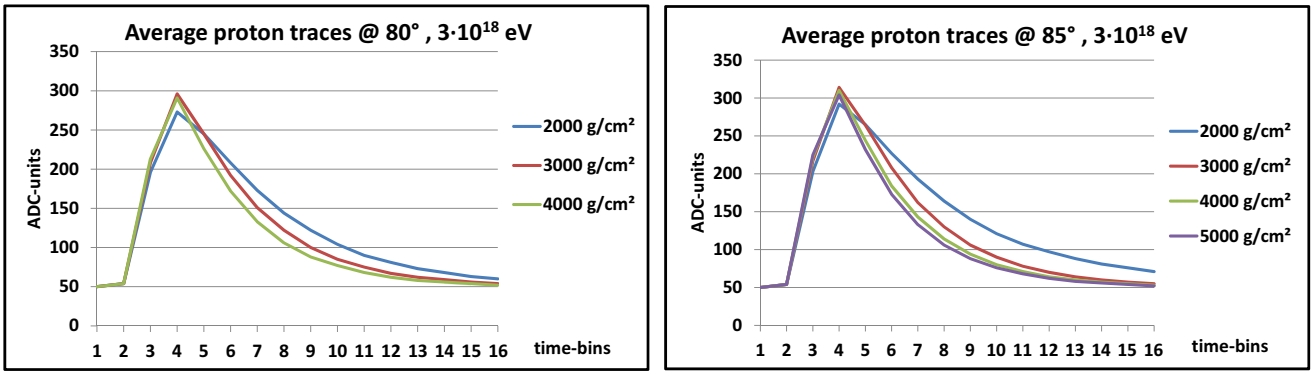

Fig. 7. Plots showing average traces for protons for different distances. As in Fig. 2 the shortest distances have different exponents than the rest.

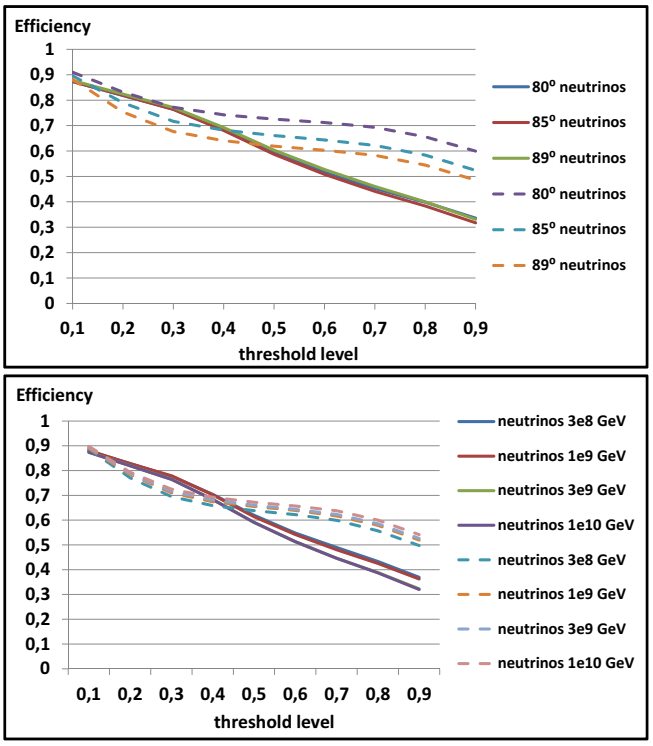

Fig. 8. The angular dependency of a neutrino efficiency as a function of a threshold level for angles (top) and energies (bottom). The continuous lines denote the data for testing were gathered from all traces. The dashed lines represent the case with separated traces.

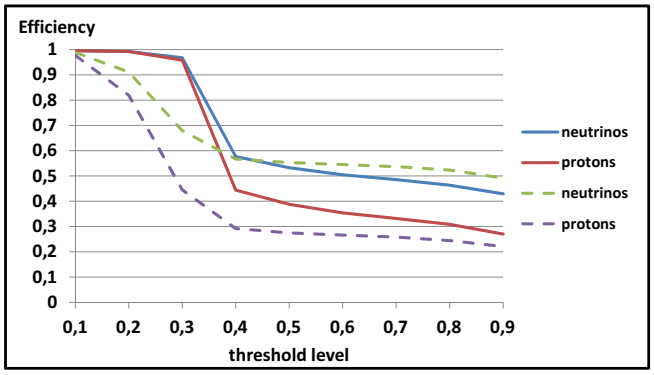

Fig. 9. The efficiency of the neutrinos recognition and proton mistakes level in function of threshold level for the non-separated (continuous lines) and separated traces (dashed lines) used for testing the ANN. The data taken for training are the same as in the Fig 8.

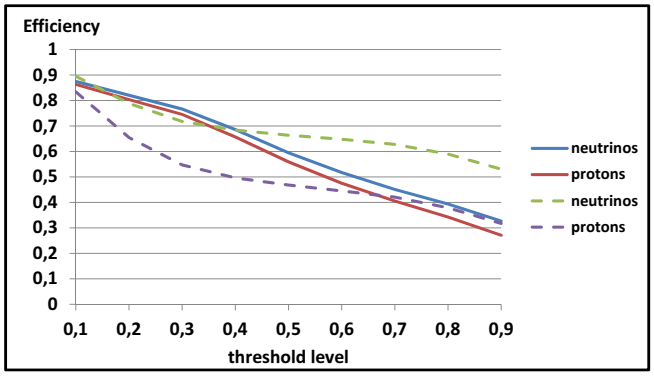

Fig. 10. The efficiency of the neutrino traces recognition and proton mistakes level in function of threshold level for the non-separated (continuous line) and separated traces (dashed line) used for testing the ANN. The traces used for training the ANN were randomly taken from all categories of non-separated or separated traces respectively.

being designed for the Front-End Board for Auger-Beyond-2015 task.

Preliminary results show that the ANN algorithm can detect neutrino events currently neglected by the standard Auger triggers.

The recognition efficiency of the neutrino traces by the ANN algorithm strongly depends on the differences between the data used for the ANN training. If we teach the ANN with the data containing only traces produced by young neutrino and old proton cosmic air showers we can reach the acceptable level of recognition. Moreover, we can distinguish protons and neutrinos, which means the ANN works on very promising level.

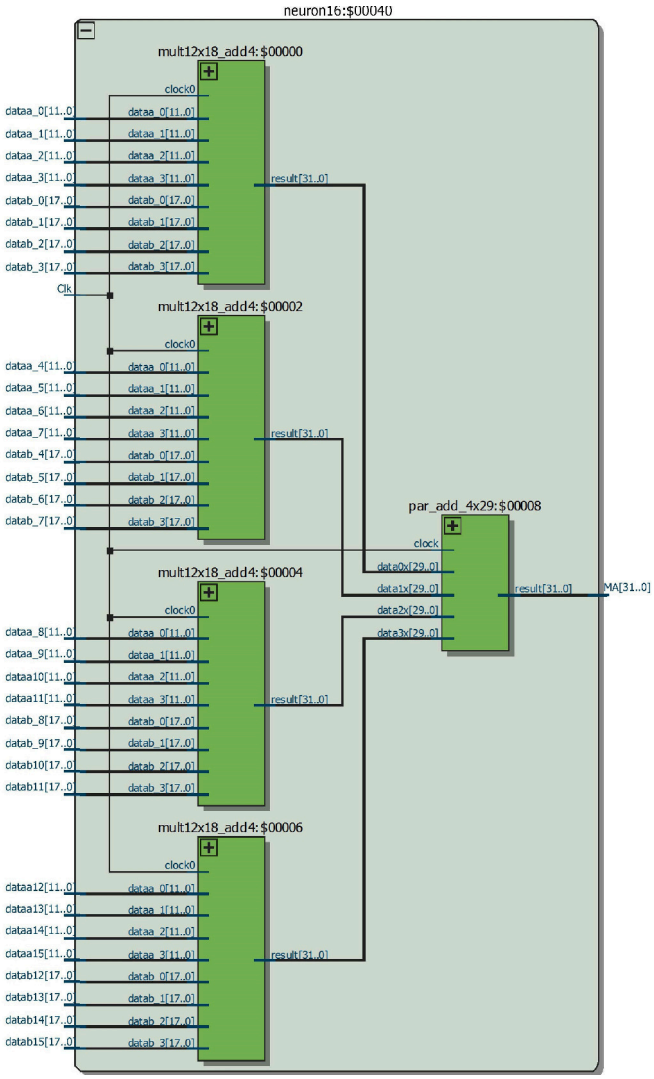

Fig. 11. An internal structure of an FPGA neuron.

ACKNOWLEDGMENT

This work is supported by the National Science Centre (Poland) under NCN Grant No. 2013/08/M/ST9/00322. Authors thank the Pierre Auger Collaboration for an opportunity of using the CORSIKA and OffLine simulation packages.

REFERENCES

[1] M. Nagano and A. A. Watson, "Observations and implications of the ultrahigh-energy cosmic rays", *Rev. of Modern Phys.*, vol. 72, no. 3, pp. 689-732, 2000.
DOI: 10.1103/RevModPhys.72.689

[2] F. Halzen and D. Hooper, "High-energy neutrino astronomy: the cosmic ray connection", *Rep. on Progress in Phys.*, vol. 65, no. 7, p. 1025, 2002.
DOI: 10.1088/0034-4885/65/7/201

[3] J. K. Becker, "High-energy neutrinos in the context of multi-messenger astrophysics", *Phys. Reports*, vol. 458, no. 4-5, pp. 173-246, 2008.
DOI: 10.1016/j.physrep.2007.10.006

[4] P. Bhattacharjee and G. Sigl, "Origin and propagation of extremely high-energy cosmic rays", *Phys. Reports*, vol. 327, no. 3-4, pp. 109-247, 2000.
DOI: 10.1016/S0370-1573(99)00101-5

[5] K. Greisen, "End to the cosmic-ray spectrum?", *Phys. Rev. Lett.*, vol. 16, pp. 748-750, 1966.
DOI: 10.1103/PhysRevLett.16.748
G. T. Zatsepin and V. A. Kuzmin, "Upper limit of the spectrum of cosmic rays", *JETP Letters*, vol. 4, p. 78, 1966.
WOS:A19668298400011

[6] [Hi-Res Fly's Eye Collaboration], "First Observation of the Greisen-Zatsepin-Kuzmin Suppression", *Phys. Rev. Lett.*, vol. 100, no. 10, article 101101, 5 pages, 2008.
DOI: 10.1103/PhysRevLett.100.101101

[7] K. Kotera, D. Allard, and A. V. Olinto, "Cosmogenic neutrinos: parameter space and detectability from PeV to ZeV", *JCAP*, vol. 2010, no. 10, article 013, 2010.
DOI: 10.1088/1475-7516/2010/10/013

[8] E. Zas, "Neutrino detection with inclined air showers", *New Journal of Phys.*, vol. 7, p. 130, 2005.
DOI: 10.1088/1367-2630/7/1/130

[9] V. S. Berezinsky, A. Yu. Smirnov, "Cosmic neutrinos of ultrahigh energies and detection possibility", *Astrophys. and Space Sci.*, vol. 32, no. 2, pp. 461-482, 1975.
DOI: 10.1007/BF00643157

[10] Z. Szadkowski, "A spectral 1^{st} level FPGA trigger for detection of very inclined showers based on a 16-point Discrete Cosine Transform for the Pierre Auger Observatory", *Nucl. Instr. Meth.*, ser. A, vol. **606**, pp. 330-343, July 2009.
DOI: 10.1016/j.nima.2009.03.255

[11] Z. Szadkowski, "Trigger Board for the Auger Surface Detector with 100 MHz Sampling and Discrete Cosine Transform", *IEEE Trans. on Nucl. Science*, vol. 58, pp. 1692-1700, Aug. 2011
DOI: 10.1109/TNS.2011.2115252

[12] Z. Szadkowski, "Optimization of the Detection of Very Inclined Showers Using a Spectral DCT Trigger in Arrays of Surface Detectors", *IEEE Trans. on Nucl. Science*, vol. 60, pp. 3647-3653, Oct. 2013
DOI: 10.1109/TNS.2013.2280639

[13] Z. Szadkowski, K. Pytel, *Artificial Neural Network as a FPGA Trigger for a Detection of Very Inclined Air Showers*, IEEE Trans. on Nucl. Science, vol. 63, Issue 3, pp. 1002-1009, June 2015.
DOI: 10.1109/TNS.2015.2421412

[14] [Pierre Auger Collaboration], "Upper limit on the diffuse flux of ultrahigh energy tau neutrinos from the Pierre Auger Observatory", *Phys. Rev. Lett.*, vol. 100, no. 21, article 211101, 2008.
DOI: 10.1103/PhysRevLett.100.211101

[15] [Pierre Auger Collaboration], "Ultrahigh Energy Neutrinos at the Pierre Auger Observatory", *Adv. in High Energy Phys.* vol. 2013, Article ID 708680, 18 pages
DOI: 10.1155/2013/708680

[16] CORSIKA an Air Shower Simulation Program [Online]. Available: https://web.ikp.kit.edu/corsika/

[17] S. Argiro et al., "The offline software framework of the Pierre Auger Observatory", *Nucl. Instrum. and Meth.* ser. A, vol. 580, Issue. 3, pp. 1485-1496, Oct. 2007.
DOI: 10.1016/j.nima.2007.07.010